



## An approach to assess the consequence of a hypothetical radionuclide release in Singapore - a densely populated urban setting

Chai Siao Yang and Xiangming Sun\*

*Singapore Nuclear Safety and Research Initiative, National University of Singapore, 1 CREATE Way, #04-01, CREATE Tower, 138602, Singapore*

\* Corresponding author, E-mail: [x.sun@nus.edu.sg](mailto:x.sun@nus.edu.sg)

**Abstract:** This study is to demonstrate an approach to investigate the consequence of a hypothetical radionuclide release scenario in Singapore, a typical urban setting with high population density. To this end, we made use of MACCS 4.1, a Gaussian-based atmospheric dispersion model to compute the peak dose and the population health effects. We developed the meteorological and site files from data provided by local government agencies. Our investigation showed that the chosen scenario poses very little to negligible risk to the health of local population as the peak dose received across the country is below the radiation safety level recommended by ICRP.

**Keywords:** *MACCS; atmospheric dispersion; Singapore; dose assessment; emergency planning.*

### I. INTRODUCTION

Atmospheric dispersion and dose assessment are key components in informing nuclear policy making, such as site assessments for hypothetical nuclear power plant (NPP), environmental assessments of existing NPPs, post-accident analysis, and etc. Various codes based on different dispersion models had been developed to simulate the atmospheric transport of radionuclide particles, such as the Hybrid Single-Particle Lagrangian Integrated Trajectory model (HYSPLIT), the Gaussian puff model ARGOS, the European RODOS/JRODOS the Japanese OSCAAR and etc. These codes are also incorporated with dose assessment tools.

On the other hand, studies of radiological impact due to hypothetical nuclear power plant (NPP) accidents had been carried out in nearby countries, such as Malaysia [1], Indonesia [2], Thailand [3], and etc. The anticipation of rapid

advancement of nuclear-related technology in Southeast Asia and Singapore's own future energy needs had thus driven us to develop our own expertise in radiological assessment.

For our preliminary investigation of potential impact of a postulated radionuclide dispersion in the urban setting of Singapore, we have chosen the MELCOR Accident Consequent Code System (MACCS) 4.1. MACCS is a Gaussian-based plume model known for its short computational time and conservative estimates with reasonable accuracy at short range (1 km – 50 km) [4]. In particular, MACCS had shown remarkable agreement with higher fidelity model such as HYSPLIT in terms of annual statistics [5], which implies that MACCS is a reliable tool for conducting probability-based radiological assessments of the aftermath of a NPP accident, customized to local population distribution and emergency planning.

Various tools had been developed to facilitate the creation of input meteorological and site files from local raw data sources in some countries, such as SecPop by USA Sandia National Laboratories and POPCON [6,7] by Korea Atomic Energy Research Institute. Our work aims to assess the potential impact of a radionuclide release event in Singapore by running MACCS with input files developed for local context.

## II. CONTENT

### A. Methodology

In this study, we primarily used the MACCS 4.1, a Gaussian-based atmospheric dispersion model developed by Sandia National Laboratories (SNL), to calculate and assess the statistical consequence of a radionuclide release due to a hypothetical accident of a light-water small modular reactor (SMR). As an illustration, the ATMOS module of MACCS performs a series of 10-day dispersion simulations using one-year worth of meteorological data of a location to calculate the concentration and deposition of the radionuclides. Subsequently, the EARLY module calculates the peak dose received from the dispersion results, and estimates the population health risks based on the population distribution data in the site file provided. To this end, we first have to preprocess local meteorological data and population data into meteorological file and site file arranged in the MACCS format.

#### *1.a. Preparation of Meteorological File*

The year of 2018 was chosen to be the time range of this study for its neutral El Niño Southern Oscillation (ENSO) conditions, implying minimal impact on Singapore's weather for most parts of the year. The relative lack of large-scale climate variability makes

2018 a good representation of Singapore's annual weather.

The surface meteorological observation data in Singapore from 2016 and onwards can be obtained from a Singapore government data portal (data.gov.sg) via API. The data we extracted include rainfall, wind, temperature and relative humidity. The rainfall is recorded as 5-minute total in units of mm, while the wind data is available at 5-minute interval for both wind direction (degree) measured from the North direction and wind speed (knots). In this study, Changi station, located at the eastern part of Singapore (1.3678 °N , 103.9826 °E ), was chosen to be the hypothetical source location as its annual rainfall and wind data are the most complete among all stations. Their percentage availabilities are 91.03% and 93.36% respectively. However, it should be noted that although the 2018 annual total rainfall across the country was close-to-average, the total rainfall recorded at Changi (before interpolation) was 1622 mm, 25% below the 1981 – 2010 long-term average, a result of the general trend that the eastern part of the island receives less rain than the northern and western parts.

The missing rain data was filled in using the data from the same time of the nearest year while the missing wind data was interpolated using the 'back fill' method, where the missing entry was filled in with that of its previous time entry.

Based on the formatting requirement of meteorological data for MACCS, we created a meteorological file containing 8760 (=365 days × 24 hours) hourly weather sequences, ended with a line specifying the morning and afternoon mixing heights extracted from the ERA5 re-analysis data set (see Section A1.2.).

**1.b. Wind rose in Singapore in 2018**

From the wind rose chart at Changi station in 2018 in Fig.1(a), Northeast wind is the predominant wind (blown from the Northeast direction), which was mainly attributed to the consistent northeasterly wind

during the Northeast monsoon that is usually experienced from December to March. The calm wind (wind speed < 0.5 m/s based on Beaufort scale from WMO) percentage and the annual wind speed average is 1.31% and 2.535 m/s respectively.

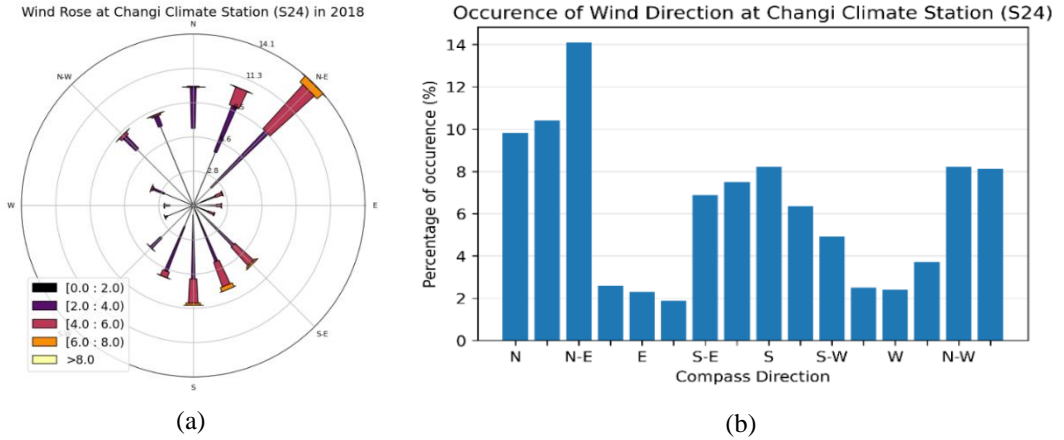


**Fig. 1.** (a) Wind rose at Changi climate station (S24) in 2018. (b) Histogram showing the frequency of each wind direction occurred over the year of 2018

**1.c. Atmospheric stability**

The meteorological data from the ERA5 re-analysis data set were also used for the stability calculation. The ERA5 data set is the state-of-the-art re-analysis data set [8] from the European Centre for Medium-range Weather Forecast (ECMWF). It combines historical observations into global estimates using advanced modelling and data assimilation systems. To determine the P-G stability categories, we followed Turner’s method [9] and used the surface winds, cloud cover and cloud ceiling from the ERA5 data set. Solar altitudes are also used in the stability calculation to determine the insolation class, which followed the Smithsonian Meteorological Tables [10] where the solar altitude was calculated from local time.

**2. Preparation of site file**

The geographical distribution of Singapore's population in terms of each subzone can be visualised by combining the census data from Singapore Census of Population and Household Survey 2020, with the demarcation of subzones based on Urban Redevelopment Authority (URA) Master Plan 2019. The population data was provided in *csv* format while the subzone data was in *geojson* format, where the subzones' shapes were encoded within. Using Python packages such as GeoPandas and Pandas, we first assigned the population data by geographical distribution to their corresponding subzones (332 in total). The functionality provided by GeoPandas allowed us to calculate the area of each subzone after choosing a suitable set of projected coordinates (EPSG), and thus the population density across Singapore. In this case, we had re-projected the data from EPSG = 4326 to EPSG = 3414.

**Table I.** Metadata of the most densely populated subzone surrounding the hypothetical source

Subzone	Latitude (°N)	Longitude (°E)	Distance from Changi Climate Station (km)	Population Density (person per km <sup>2</sup> )
JURONG WEST CENTRAL	1.340	103.702	31.366	45396
YEW TEE	1.401	103.748	26.367	43749
TIONG BAHRU STATION	1.284	103.827	19.656	43103
SENGKANG TOWN CENTRE	1.392	103.898	9.810	42306
FAJAR	1.385	103.771	23.607	41618
PENG SIANG	1.379	103.739	27.181	40244
WOODLANDS EAST	1.441	103.802	21.685	38763
TOWNSVILLE	1.365	103.848	14.929	38690
SAUJANA	1.386	103.766	24.162	38400
RIVERVALE	1.388	103.905	8.909	38049

To arrange the population data into the format required by MACCS, we first generated square grids over the map of Singapore and assigned each of them with population based on the intersection of subzones with them, using the area-ratio method. The idea is summarised by the following equation,

$$N_i = \sum_s N_s \times \frac{A_{\text{int}(i,s)}}{A_s} \quad (1)$$

Where  $N_i$  is the population number in cell  $i$ ,  $N_s$  is the population number of a particular subzone  $s$ ,  $A_{\text{int}(i,s)}$  is the intersection area between cell  $i$  and subzone  $s$  and  $A_s$  is the area of the subzone  $s$ . This means that the population number in a grid cell is the sum of population number of the intersecting subzones weighted by their respective ratios of intersection area to subzone area.

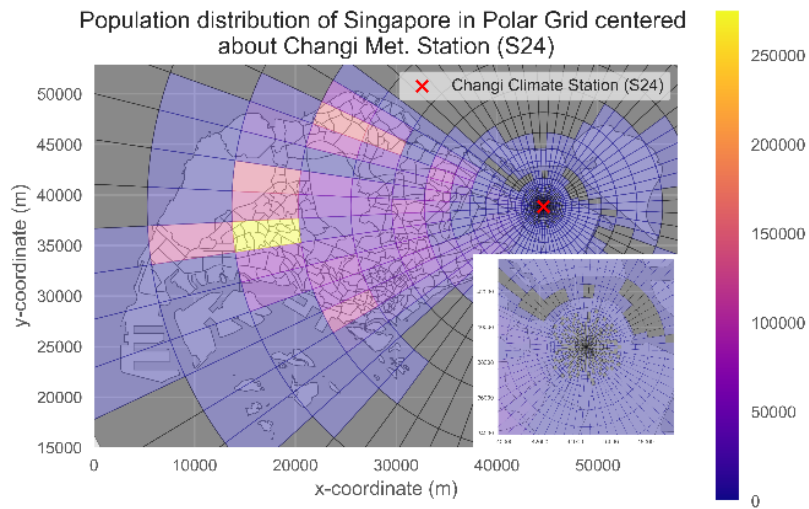


**Fig. 2.** Population distribution in Singapore expressed in MACCS polar coordinate system. The inset shows the polar elements in radial rings within 2 km from the center

Since MACCS is using a polar coordinate system centering around the source location, we assigned the population data in the square grid cells to the polar element they belong to, based on the element's centroid's polar coordinates relative to Changi station, by computing its radial distance and polar angle using trigonometric formulas. The results of this population assignment are shown in Fig. 2.

Finally, they were written into a text file to be used as the input for our MACCS simulation.

### 3. Accident scenario selection (source term)

We used a toy source term of a hypothetical accident light water small modular reactor (SMR), developed by our Safety Analysis team using MELCOR and preprocessed using MelMACCS, which was still a work in progress. In this scenario, there are 10 plumes released in total, each of them lasted an hour, except the last one which was 20 minutes. The total released radioactivity is  $4.38 \times 10^{12}$  Bq. The full core inventory is not disclosed here as an in-depth discussion of it is beyond the scope of this paper.

### 4. Configuration and assumptions

We used the stratified random sampling method with number of samples per day (NSMPLS) set to 24, which means that each of the weather sequences specified in the meteorological file will be sampled as the initiation time of the accident to calculate their respective resultant doses to the public and health risks after 10 days (8760 trials for each simulation). A cumulative distribution function (CCDF) is generated over all these trials at the end of all the calculations to provide an overall statistical representation of the effects of the accident for the year of 2018. For the

purpose of setting up a control for our future work, we assumed that the population is nonevacuating in this simulation. The numerical results were then post-processed to produce graphical visualisations of the consequences across the country.

## B. Results

In this study, we focused on the peak dose and population-weighted cancer risk incurred due to the accident, by considering their median and peak consequence. The median refers to the middle value of all the 8760 trials, whereas the peak consequence is the highest possible value incurred among all those trials.

Fig. 3 shows the composite result of median peak dose received by a representative individual in each of the polar elements. Meanwhile, the peak values are presented in Fig. 4. For both measures, the highest values are found in the innermost ring (0 - 0.2 km), generally in the southwestern direction of the hypothetical source. The peak consequence value is 0.733 mSv, which is around 2 orders of magnitude larger than the median value at  $2.28 \times 10^{-3}$  mSv.

By intersecting the MACCS results in polar coordinates with Singapore subzones, we obtained Fig. 5 which represents the highest possible peak dose each subzone can receive. The bar chart in Fig. 6 shows some other most heavily affected subzones in terms of peak dose received, with Changi Airport and Changi West tie at the top spot with 0.733 mSv received as both locations are in immediate proximity of the first radial ring. The subsequent subzones that intersect with the outer rings receiving significantly less amount of peak dose, i.e.  $\leq 0.166$  mSv. Unsurprisingly, all these subzones are located at the east side of Singapore.

AN APPROACH TO ASSESS THE CONSEQUENCE OF A HYPOTHETICAL RADIONUCLIDE...

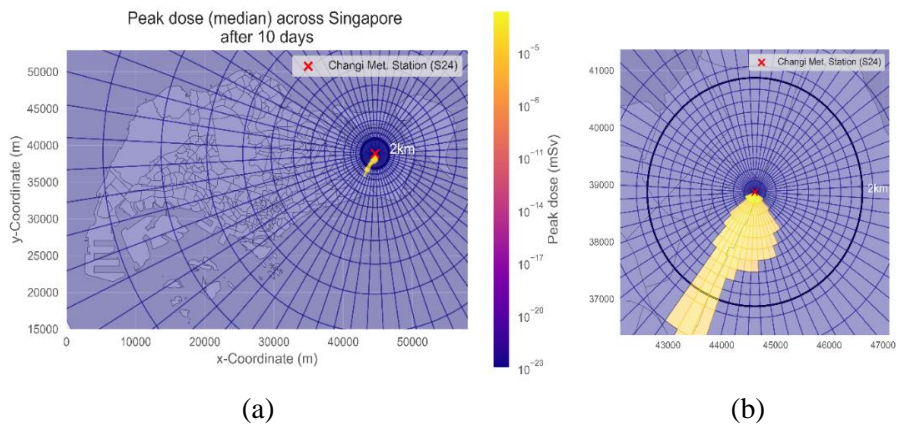


**Fig. 3.** (a) The overlay of median peak dose results over the map of subzone of Singapore. (b) Median peak dose results within 2 km from the hypothetical source location.

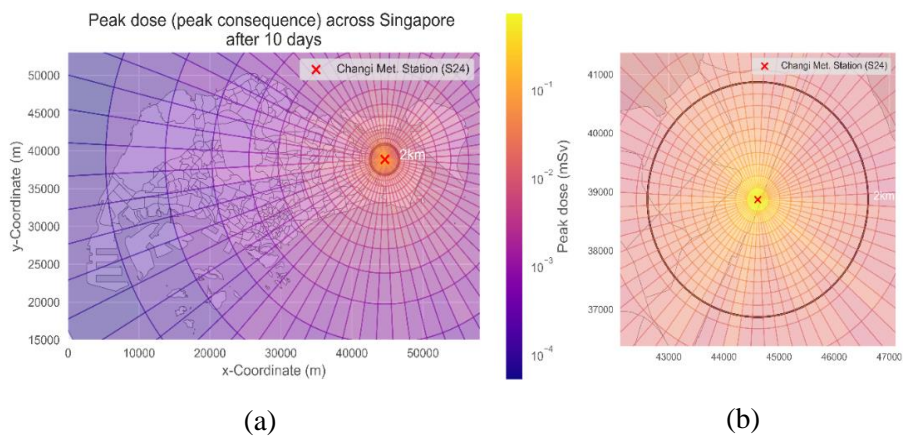


**Fig. 4.** (a) The overlay of peak consequence among peak dose results over the map of subzone of Singapore. (b) Peak consequence among peak dose results within 2 km from the hypothetical source location

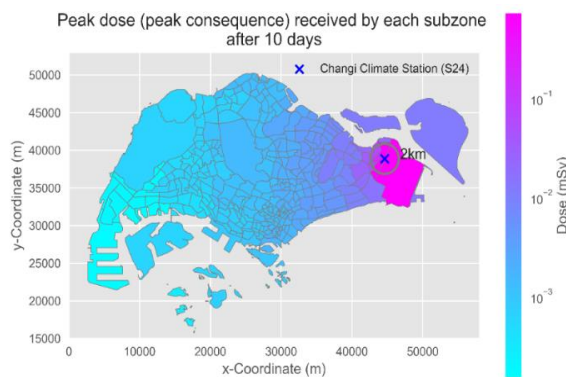


**Fig. 5.** The dose map across subzones in Singapore, produced by first finding the intersections between the polar elements and the subzones. Each subzone is then assigned with the highest peak dose value among the polar elements that intersect with it

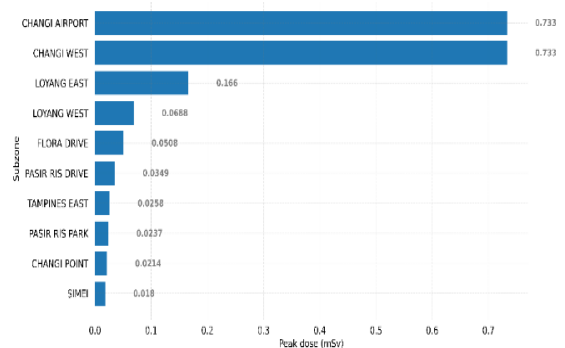


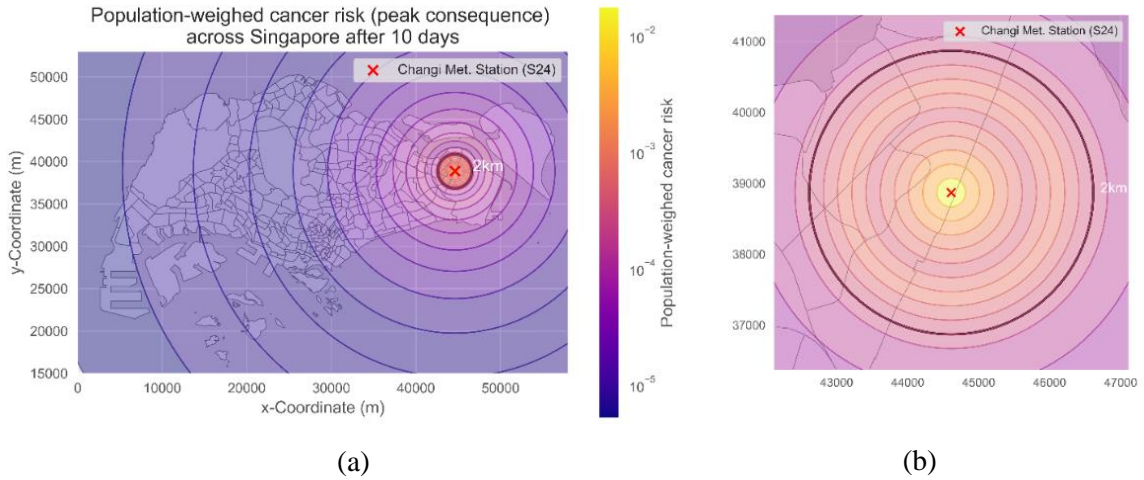
**Fig. 6.** Subzones receiving the highest peak dose (peak consequence) 10 days after the time of release

On the other hand, the population-weighted cancer risk in a particular ring is calculated with the formula:

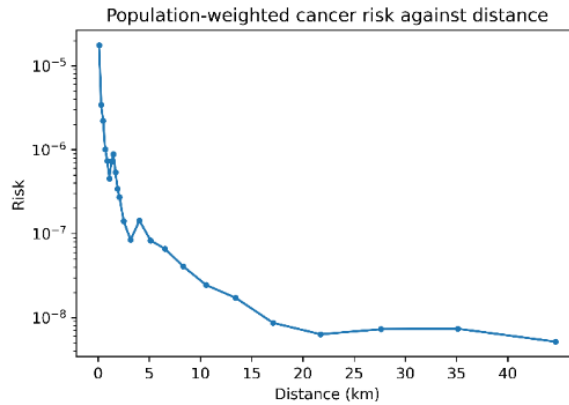
$$Risk = \frac{\text{Number of cancer cases in the polar ring}}{\text{Population in the polar ring}} \quad (2)$$

Fig. 7 shows that the population-weighted cancer health risk is the highest in the

innermost ring, with the value of  $1.76 \times 10^{-5}$  per person or around 2 cases per 100,000 people. Fig. 8 depicts general decrement of the risk as one moves away from the source location along the radial direction, with small rebounds observed between Zone 5 (0.8 – 1.0 km) and 8 (1.4 – 1.6 km), 13 (2.8 – 3.6 km) and 15 (4.5 – 5.8 km), 21 (19.1 – 24.3 km) and 24 (39.3 – 50.0 km).



**Fig. 7.** (a) The overlay of population-weighted cancer risk results over the map of subzone of Singapore. (b) Peak consequence of population-weighted cancer risk results within 2 km from the hypothetical source location



**Fig. 8.** Plot of population-weighted cancer risk against distance from the center point of each radial ring to the source location)

**C. Discussion**

The peak consequence result of peak dose can be considered as the worst-case

scenario. This is because it is the highest possible dose one could receive at a particular location given that the accident sequence

begins at a particular hour in a year with a certain weather condition. In this study, the peak consequence has a probability of occurrence of  $1/8760$  or  $1.142 \times 10^{-4}$ . We found that the highest value incurred for this particular source term is 0.733 mSv, below the annual public dose limit (on top of background doses) recommended by ICRP, which is 1 mSv/yr. However, it should be noted that the core inventory considered here is not fully developed, thus it is an underestimation of the actual output of an SMR accident.

On the other hand, we observed that the polar elements in the southwestern direction of the source generally receive higher median peak doses than those in the other directions, showing correlation with the wind rose, where the northeast wind (which blown towards the SW direction) had the highest frequency of occurrence.

On the small bumps observed in Fig. 8, the dose decreases as one moves away from the source radially, the number of cancer cases estimated in the farther polar rings should be decreasing in general. Therefore, the rebounds should be attributed to the decrease in the denominator of Eqn. (2), that is, the population residing within those polar rings are relatively lower.

### III. CONCLUSION

In this paper, we have demonstrated an approach to assess the consequence of a hypothetical radionuclide release accident in a densely-populated urban setting. We had simulated the dispersion of radionuclides using a Gaussian-based model and conducted a spatial analysis of the potential health risk posed to Singapore population using local meteorological and population data.

As a closing note, this work will be used as a precursor to future work to advise site assessments and determinations of a suitable emergency planning zone (EPZ) for potential NPP of SMR type in densely populated cities, by utilising a more fully developed source term from MELCOR. We will also work on developing a meteorological file with a more representative dataset of Singapore's weather conditions, using 5- or 10-years meteorological data provided by local agencies.

### ACKNOWLEDGMENTS

The authors express their gratitude to their colleagues Tan Tu Guang, Tang Jia Hao, Issac Yap Ching Hiong and Vitesh Krishnan in the Nuclear Safety Analysis Team for developing and providing the source term to us for this study.

### REFERENCES

- [1]. Omar, N., Koh, M-H., Hashim, S., "Radiological dose assessment due to hypothetical nuclear power plant operation in Mersing, Johor, Malaysia". Malaysian Journal of Fundamental and Applied Science., 2019, 15, (4), pp. 532-536.
- [2]. Rosli, R., et al., "Atmospheric trajectory analysis of Cesium-137 from proposed nuclear power plant site in Bangka Island, Indonesia". J. Phys.: Conf. Ser., 2021, 2053, 012010.
- [3]. Silva, K., et al., "Preliminary results of consequence assessment of a hypothetical severe accident using Thai meteorological data". J. Phys.: Conf. Ser., 2017, 860, 012039.
- [4]. Bogorad, V., Lytvynska, T. , Bielov, Ia., "Comparative analysis of calculation possibilities of MACCS and RODOS computer codes for tasks of emergency response and analysis of radiation consequences of severe accidents at NPPs". Nuclear and Radiation Safety, 2017, 1, (73), pp. 56-61.



- [5]. Clayton, D.J., Bixler, N.E., Compton, K.L., “HYSPLIT/MACCS Atmospheric Dispersion Model Technical Documentation and Benchmark Analysis”. Sandia Report/SAND2022-5515, Sandia National Laboratories, April 2022.
- [6]. Jang, S-C., Kim, S-Y., Lee, S-H., “Development of the GIS-based Population Data Conversion Program, POPCON”. Transaction of the Korean Nuclear Society Virtual Spring Meeting, Jeju, Korea, May 13-14, 2021.
- [7]. Park, H., Kim, S-Y., Jang, S-C., “Validation & Verification of GIS-Based Population Data Conversion Program (POPCON)”. Transaction of the Korean Nuclear Society Virtual Spring Meeting, Jeju, Korea, May 13-14, 2021.
- [8]. Hersbach, H, et. al., The ERA5 global reanalysis, Q. J. R. Meteorol. Soc., 2020, 146, pp. 1999-2049.
- [9]. Turner, D.B., A diffusion model for an urban area. J. Appl. Meteor., 1964, 3. pp. 83-91. U.S. Environmental Protection Agency, (EPA), “White Paper on Bt plant-pesticide resistance management”. (Publication 739-S-98-001, EPA, 1998;
- [10]. List, R. J. 1966. Smithsonian Meteorological Tables, Sixth Revised Edition (Third Reprint). Smithsonian Institution, Washington, D. C.